Chronic brain inflammation and persistent herpes simplex virus 1 thymidine kinase expression in survivors of syngeneic glioma treated by adenovirus-mediated gene therapy: Implications for clinical trials

R. A. Dewey, G. Morrissey[1], C. M. Cowsill[1], D. Stone[1], F. Bolognani[1], N.J.F. Dodd[2], T. D. Southgate[1], D. Klatzmann[3], H. Lassmann[4], M.G. Castro[1] & P.R. Löwenstein[1]

[1]*Molecular Medicine and Gene Therapy Unit, Room 1.302 Stopford Building, School of Medicine,*
[2]*Department of Medical Biophysics, Stopford Building, University of Manchester, Oxford Road, Manchester M13 9PT, UK*
[3]*Laboratoire de Biologie et Therapeutique des Pathologies Immunitaires, Universitè Pierre et Marie Curie, CNRS, Hôpital de la Pitiè-Salpétrière, 83 Boulevard de l'Hôpital, 75651, Paris Cedex 13, France*
[4]*Neurological Institute, University of Vienna, Schwarzspanierstrasse 17, A-1090 Vienna, Austria*
R.A.D present address: Department of Neuropathology, Institute of Psychiatry, Kings College London, DeCrespigny Park, Denmark Hill, London SE5 8AS, UK
R.A.D., G.M. and C.M.C. contributed equally to this study.
Correspondence should be addressed to P.R.L.; email: lowenstein@man.ac.uk, or M.G.C.; email: mcastro@fs1.scg.man.ac.ul

The long-term consequences of adenovirus-mediated conditional cytotoxic gene therapy for gliomas remain uncharacterized. We report here detection of active brain inflammation 3 months after successful inhibition of syngeneic glioma growth. The inflammatory infiltrate consisted of activated macrophages/microglia and astrocytes, and T lymphocytes positive for leucosyalin, CD3 and CD8, and included secondary demyelination. We detected strong widespread herpes simplex virus 1 thymidine kinase immunoreactivity and vector genomes throughout large areas of the brain. Thus, patient evaluation and the design of clinical trials in ongoing and future gene therapy for brain glioblastoma must address not only tumor-killing efficiency, but also long-term active brain inflammation, loss of myelin fibers and persistent transgene expression.

Clinical trials of conditional cytotoxic gene therapy of glioblastoma are now underway using retroviral and adenoviral vectors encoding herpes simplex virus 1 thymidine kinase (HSV-1-TK), followed by the administration of ganciclovir[1–4]. Much of the efficiency of suicide-gene therapy is thought to be due to the 'bystander effect', of which inflammation and anti-tumor immune stimulation seem essential components[5–7]. Despite many experimental studies examining the efficiency of glioma regression induced by suicide-gene therapy[8–17], there is no information on the incidence of subsequent chronic brain inflammation. Gene transfer into the brain using adenoviral vectors induces acute, short-lived, inflammatory reactions[18–20], although peripheral re-administration of viral vectors induces a delayed-type hypersensitivity reaction[19], which eliminates transgene expression, and is accompanied by localized demyelination. Likewise, most transgenic protein expression is mostly, although not exclusively, restricted to the injection site and is detectable for at least 2 months[18,19,21–24]. Understanding the long-term consequences of suicide gene therapy of brain tumors is thus essential.

We assessed the long-term outcomes of adenovirus-mediated conditionally cytotoxic gene therapy (that is, the combination of a pro-drug-converting enzyme encloded by the viral vector, and a pro-drug that can be administered systemically) in a syngeneic glioblastoma model. We implanted CNS-1 cells[25] into the striata of Lewis rats, and then injected adenovirus expressing HSV-1-TK, and systemic ganciclovir. The treatment was very efficient, resulting in the survival of 80–100% of rats for at least 3 months. Unexpectedly, the brains of long-term survivors showed the presence of chronically active brain inflammation, as well as very strong and widespread HSV-1-TK immunoreactivity. These data have implications for the design and evaluation of clinical gene therapy trials of glioblastoma multiforme.

HSV-1-TK /ganciclovir inhibits syngeneic CNS-1 glioma growth

Implantation of 5×10^3 CNS-1 cells unilaterally into the striatum of Lewis rats killed the rats within 30 days (Fig. 1). Injection of 8×10^7 infectious units (IU) of a replication-defective recombinant adenovirus (RAd) expressing either the full-length gene for HSV-1-TK (RAd-128), or a truncated, biologically active gene for HSV-1-TK of reduced intrinsic toxicity[26–27], HSV-1-ΔTK (RAd-127), into the same site at 3 days after implantation, followed by ganciclovir treatment for 7 days, almost completely inhibited CNS-1 glioma growth. We monitored rats by weekly magnetic resonance imaging brain scans to assess treatment effectiveness. We found tumor growth only in a single rat treated with RAd-127. There was no magnetic resonance imaging, clinical or anatomical evidence of tumor growth in any other rats. Survival at 3 months after tumor implantation was 100% in rats injected with RAd-128 and 83–100% in rats injected

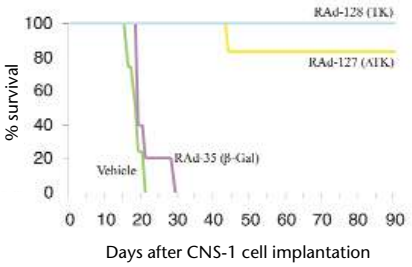

Fig. 1 Survival analysis. Lewis rats were implanted with CNS-1 cells and treated with RAd-128 (TK), RAd-127 (ΔTK), RAd–35 (βgal) or vehicle, and ganciclovir. Rats treated with RAd-128 and RAd-127 survived longer than the other two groups. There were no statistically significant differences between rats treated with vehicle and RAd-35, or between rats treated with RAd-128 and RAd-127.

with RAd-127 (survival of rats injected with RAd-127 in Fig. 1 was 83%). The survival rates of rats injected with either RAd-128 or RAd-127 were significantly better than of those of rats treated with either RAd-35, an adenovirus vector expressing β-galactosidase, or vehicle alone ($P = 0.0079$). There were no significant differences in survival either between groups treated with vehicle or RAd-35 ($P = 0.1232$), or between groups treated with RAd-128 or RAd-127 ($P = 0.3613$). In two identical repeat experiments, we detected no tumor growth in rats treated with either RAd128 or RAd127.

General histopathological analysis

We perfusion-fixed long-term (90 days) survivors in our experimental syngeneic glioma trials, and analyzed their brains histopathologically for the distribution of glial, inflammatory, and immune cell markers, as well as for the integrity of myelin fibers and oligodendrocytes. Sections stained with hematoxylin and eosin showed the presence of inflammatory infiltrates (diffuse hypercellularity within the white matter, striatum and perivascular cuffs), and lateral ventricle enlargement (also detected by magnetic resonance imaging) ipsilateral to tumor and viral vector injection (Fig. 2*a* and *b*).

Astrocytosis

Immunohistochemical staining for the astrocyte markers vimentin (Fig. 2*c* and *d*) and glial fibrillary acidic protein (GFAP) (Fig. 2*e* and *f*) indicated widespread activation of astrocytes. GFAP is expressed by astrocytes, and is upregulated after activation. Vimentin is undetectable in resting adult rodent astrocytes, but is also upregulated after activation. Astrocyte activation was bilateral, but was strongest in the ipsilateral subcortical white matter. Vimentin-positive cells had typical astrocytic morphology, with perivascular end-feet. The distribution of activated GFAP immunoreactive astrocytes was much wider than the area occupied by vimentin-immunopositive cells. Astrocyte activation was present in all rats.

Microglial/macrophage activation and lymphocyte infiltration

Activated ED1 immunoreactive macrophages/microglia, showing ongoing phagocytosis (that is, containing tissue debris), were present mainly ipsilaterally, over a more restricted area than that occupied by activated astrocytes (Fig. 2*g* and *h*). Within the ipsilateral subcortical white matter, the area occupied by ED1$^+$, CD3$^+$, leucosyalin-positive, or CD8$^+$ cells overlapped with the hypercellularity detected in the sections stained with hematoxylin and eosin, GFAP or vimentin (Fig. 2). In the striatum, activated microglia/macrophages were found surrounding the needle track, and infiltrating trans-striatal white matter tracts. Activated microglia/macrophages were distributed throughout the dorsal and ventral subcortical white matter, the corpus callosum, and the ipsilateral anterior commissure. Only very few could be detected in the contralateral subcortical white matter (Fig. 3*e* and *f*). Activated microglial/macrophages were also found within perivascular cuffs (Fig. 3*g*), with leucosyalin-positive, CD3$^+$ and CD8$^+$ lymphocytes (Fig. 3*h*). Lymphocytes were also present within the ipsilateral subcortical white matter, as well as infiltrating striatal tissue (Fig. 3*i* and *l*).

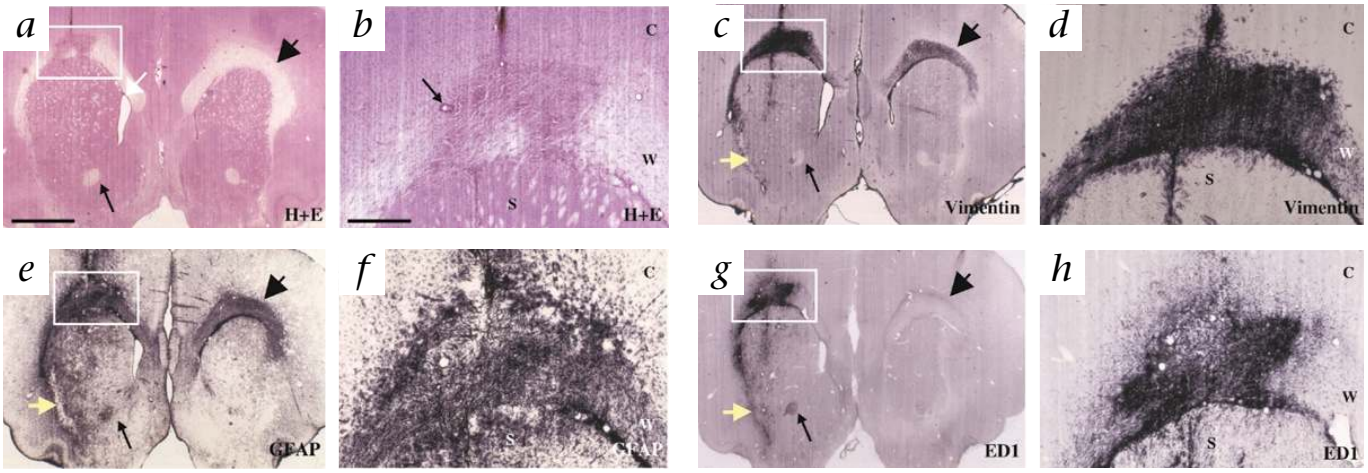

Fig. 2 Brain inflammation in long-term survivors of suicide-gene therapy. CNS-1 tumor cells and virus were injected into the right hemisphere (left side, *a,c,e,g*); adjacent sections 70 mm in thickness were analyzed. Right column, higher magnification of areas boxed in left column. Large black arrowheads, contralateral subcortical white matter; large yellow arrows, ipsilateral subcortical white matter; long thin black arrows (*a,c,e,g*), anterior commissure. C, cortex; W, white matter; S, striatum. ***a*** and ***b***, Staining with hematoxylin and eosin shows inflammatory infiltration of subcortical white matter; this demonstrates the widespread inflammatory infiltrate, and perivascular cuffs (thin black arrow, *b*). White arrow (*a*), dilated ventricle in the tumor-treated hemisphere. ***c–f***, Atrocytes immunoreactive to vimentin (*c* and *d*) and GFAP (*e* and *f*) show bilateral activation, with the highest degree of activation ipsilateral to the tumor and viral vector administration. Glial activation extends throughout the ipsilateral subcortical white matter towards its ventral extension, and is also present in the contralateral subcortical white matter. The infiltration in the ipsilateral white matter extends further than that seen in *a* and *b*. ***g*** and ***h***, The distribution of activated macrophage/microglial ED1-positive cells, present exclusively in the ipsilateral hemisphere; only low numbers of ED1-positive cells are present in the contralateral subcortical white matter (Fig. 3*e* and *f*). ED1 immunoreactivity extends to the ventral extension of the ipsilateral subcortical white matter (large yellow arrow), and also encompasses the anterior commissure (long thin black arrow). No ED1-immunoreactive cells are present in the contralateral cortex, or striatum. Scale bars represent 2 mm (left column; in *a*) and 500 μm (right column; in *b*).

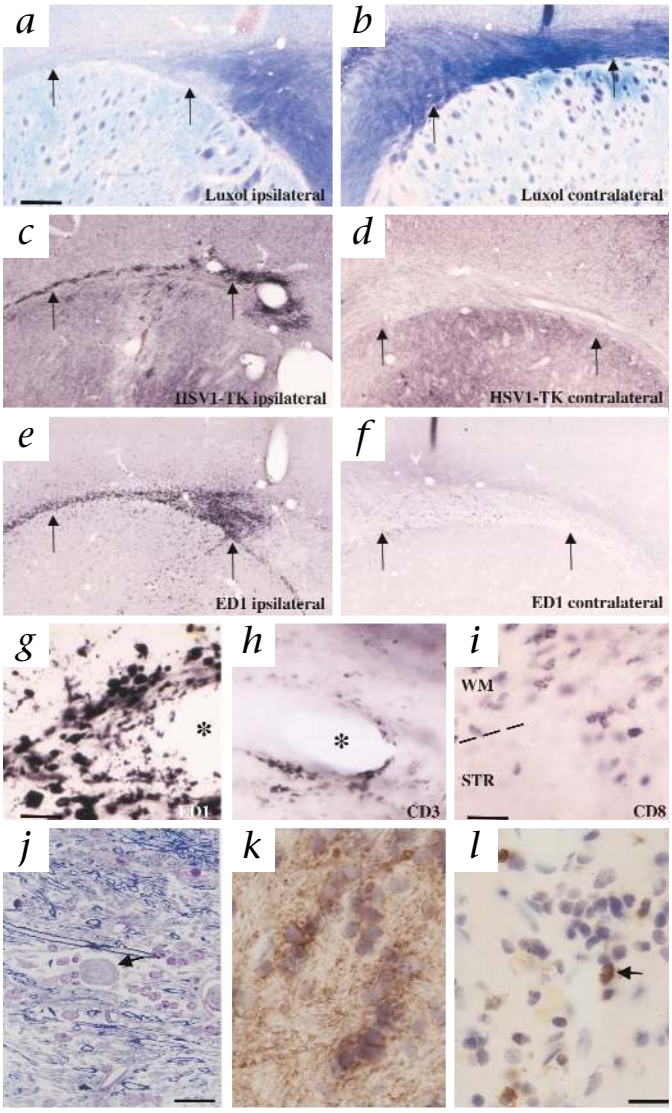

Fig. 3 Loss of myelinated fibers, HSV-1-TK immunoreactivity and macrophage and lymphocyte infiltration of perivascular cuffs. The decrease in myelinated fibers in long term suicide-gene therapy survivors is not due to autoimmune destruction of oligodendrocytes. Upward thin black arrows, subcortical white matter. ***a*** and ***b***, Sections stained with luxol fast blue show the white matter loss of myelinated fibers, which is most clearly demonstrated in the subcortical white matter in the ipsilateral hemisphere. ***c*** and ***d***, The expression of HSV-1-TK immunoreactivity in the ipsilateral (*c*) and contralateral (*d*) hemisphere indicates the continued presence of strong transgene positivity in both the ipsilateral and contralateral hemispheres. In the ipsilateral hemisphere, there is high expression of HSV-1-TK immunoreactivity in cells within the subcortical white matter, striatum and cortex. In the contralateral hemisphere, HSV-1-TK immunoreactivity in the white matter and striatum is found mainly in axons, whereas in the neocortex HSV-1-TK immunoreactivity is localised to neurons and axonal processes. ***e*** and ***f***, ED1-immunoreactive cells demonstrate the more widespread distribution of activated macrophages in the ipsilateral hemisphere, extending both into the cortex, and throughout the striatum (*e*); in the contralateral hemisphere (*f*), ED1 immunoreactive cells are present only in the white matter, but not in the cortex or striatum. ***g*** and ***h***, High-power magnification of a subcortical white matter perivascular cuffs, showing that both macrophages (*g*) and CD3-immunoreactive lymphocytes (*h*) are present. *, blood vessel lumen. ***i***, CD8-immunoreactive lymphocytes are present throughout the subcortical white matter and infiltrate the striatum. WM, white matter; STR, striatum; dashed line, border between these. ***j***, High-power magnification of a semithin Epon section, stained with osmium tetroxide and toluidine blue, showing reduced density of myelin fibers throughout the white matter. The decrease in the density of myelinated fibers is accompanied by an increase in white matter cellularity and extracellular space due to edema.Black arrow, axonal spheroid, indicative of axonal degeneration. ***k***, Oligodendrocytes, specifically stained with antibodies against CNPase. ***l***, Leucosyalin-positive T cells (two indicated by black arrow) are present in the white matter–striatal junction in the injected hemisphere. The decrease in the density of myelinated fibers, the absence of primary selectively demyelinated axons, the presence of large numbers of oligodendrocytes, and evidence of axonal degeneration, demonstrate that the loss of myelinated fibers is secondary, rather than primary immune-mediated. Scale bars represent 350 μm (for *a–f*; shown in *a*), 35 μm (for *g* and *h*; shown in *g*, 40 μm (for *i*), 50 μm (for *j*) and 30 μm (for *k* and *l*; shown in *l*).

Loss of myelinated fibers

The loss of Luxol fast blue staining strongly indicated a substantial reduction of myelinated fibers in the ipsilateral subcortical white matter (Fig. 3*a* and *b*), which spread into its ventral extension. Luxol fast blue staining was less intense in the injected striatum than in the contralateral side, indicating actual loss of myelinated fibers within the striatum as well. 'Semi-thin' Epon-embedded sections (Fig. 3*j*), stained with osmium and toluidine blue to highlight myelinated fibers, confirmed the loss of myelinated fibers within the subcortical white matter. This also indicated the presence of increased extracellular space (due to fiber loss and edema), and an increase in cellularity, composed mostly of astrocytes and oligodendrocytes (Fig. 3*j–l*). The reduced density of myelinated fibers, the presence of oligodendrocytes (identified using specific CNPase antibodies; Fig. 3*k*), with the absence of primary demyelinated axons, strongly indicates that the loss of myelin fibers is secondary to tissue degeneration, rather than due to primary immune-mediated demyelination. The presence of axonal spheroids (Fig. 3*j*) further indicates ongoing axonal degeneration.

Long-term presence of immunoreactive HSV-1-TK transgene

We assessed the presence of HSV-1-TK immunoreactivity in the brains of rats surviving tumor gene therapy for 3 months. Unexpectedly, we detected very strong and widespread immunoreactivity (Figs. 3*c* and *d*, 4 and 5*a*). In the ipsilateral hemisphere, there was strong immunoreactivity in an area overlapping the distribution of ED1$^+$ microglia/macrophages within the subcortical white matter. Furthermore, we detected strong HSV-1-TK immunoreactivity throughout the ipsilateral striatum, both in neurons and axonal processes, as well as throughout the contralateral hemisphere (Figs. 4 and 5*a*).

Many HSV-1-TK-immunoreactive neurons, axons and synaptic boutons were distributed throughout substantial areas of the ipsilateral and contralateral cortex (Figs. 3*c* and *d*, 4*a* and *c* and 5*a*). Immunoreactive neurons were mainly of pyramidal morphology, and were concentrated in layers II/III and V (Fig. 4 *a-c*). This strongly indicates that cortico–cortically projecting neurons contain high levels of HSV-1 TK protein. Brain areas with many strongly immunoreactive HSV-1-TK neurons throughout the contralateral hemisphere (outside of the subcortical white matter) proved to be completely devoid of any ED1-positive activated macrophages, or CD3/CD8-positive lymphocytes (Figs. 2*g* and 3*e* and *f*). Contralateral striata only contained many HSV-1-TK-immunoreactive axons (Figs. 3*d* and 5*a*). These most likely represent axons of cortical neurons projecting to lower levels of the neuraxis. Although there was strong labeling in all rats examined, the distribution of labeled cells varied between rats.

To exclude the possibility of any nonspecific immunoreactivity, we used the following controls: Sections from rats injected with

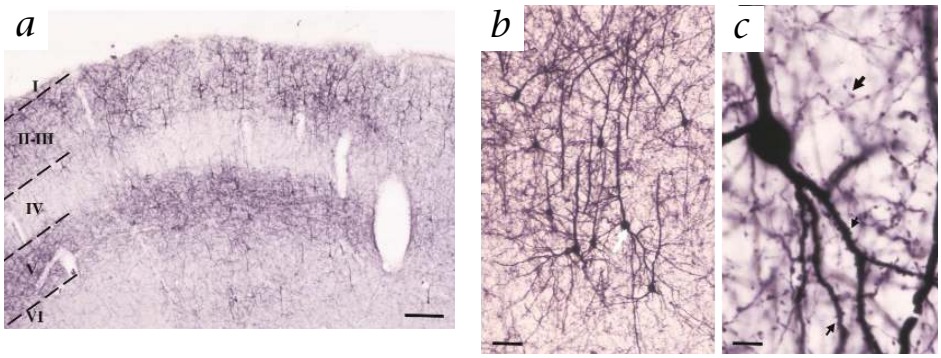

Fig. 4 Persistence of HSV-1-TK within neurons in long-term survivors of suicide-gene therapy. ***a***, Somatosensory cortex contralateral to the original injection site in a 3 month survivor (low-power magnification), showing strong labeling of pyramidal cells in layers II–III, and labeling of cells and axonal processes in layer V. ***b***, High-power magnification of pyramidal cells, showing the pyramidal morphology and very strong labeling of both apical and basal dendrites. These most likely correspond to retrogradely labeled pyramidal cells. ***c***, Higher-power magnification of the pyramidal cell indicated by a white arrow in *b*, showing strong immunoreactivity of the cell body, the apical and basal dendrites. Small black arrows, labeling in dendritic spines; thicker arrow, labeled immunoreactive axonal boutons. No indication of pathology in HSV-1-TK-immunoreactive neurons could be detected. Scale bars represent 235 μm (*a*), 50 μm (*b*) and 10 μm (*c*).

RAd-127 or RAd-128 and ganciclovir were immunoreacted with secondary antibodies in the absence of primary antibodies. There was no positive staining, indicating that the secondary antibodies were not cross-reacting with nonspecific tissue components. Sections from rats treated with RAd35 and ganciclovir or with vehicle and ganciclovir were immunoreacted with primary antibody against HSV-1-TK and secondary antibodies. There was no immunopositivity. This excludes the possibility that virus and/or ganciclovir injection might induce the production of an endogenous protein detected by antibodies against HSV-1-TK. Also, we tested viral stocks before injection using the supernatant rescue assay; these were devoid of replication-competent adenovirus. To confirm that no very low-level contamination could have been amplified in the brain during the three months of the experiment, we devised a PCR-based method to detect the presence of any replication-competent virus in the brain. Three regions of the viral genome were amplified by PCR from the same brain sections used for immunohistochemistry (Fig. 5*b* and *c*). The IVa2 region is present in the genome of vectors and in the genome of any replication competent virus. The E1B region is present in the genome of a replication-competent virus and in 293 cells, but not in the E1-deleted vectors. TK sequences will be present only in RAd127 and RAd128, and we used a β-actin sequence as a control for DNA extraction.

We amplified the TK and the IVa2 region, but not the E1B fragment, from sections of brains injected with either viral vector 3 months earlier (Fig. 5*b*). This demonstrates that vector genomes, but not replication-competent viral genomes, were present. To confirm that the E1B fragment, if present, could be amplified from brain tissue, we injected a preparation of an unrelated viral vector contaminated with replication-competent adenovirus (as assessed using the supernatant rescue assay) into the brain. From sections taken from such brains, we amplified both the IVa2 and the E1B region, as expected (Fig. 5*b*).

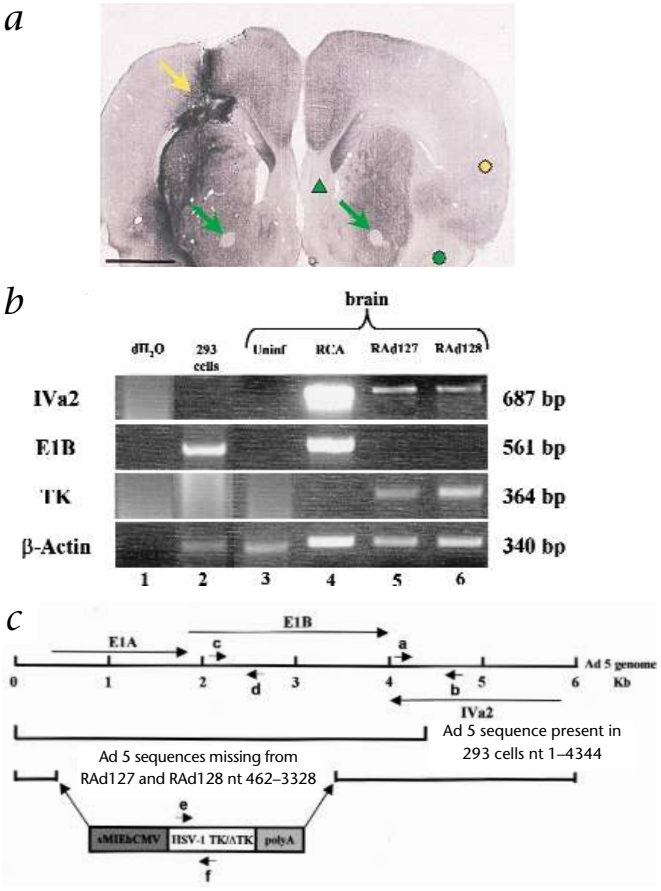

Fig. 5 PCR analysis of brain sections from long-term survivors of suicide-gene therapy. ***a***, Immunohistochemical staining for HSV-1-TK in a 3-month survivor, in a coronal section. Yellow arrow, staining around the injection site; yellow circle, area in the contralateral cortex with many HSV-1 TK immunoreactive cell bodies and axons. All of the darkly stained areas in this section contain HSV-1-TK-immunoreactive structures. Green arrows, lack of staining in the ipsilateral and contralateral anterior commissures; green triangle and circle, lack of staining in the septum and contralateral piriform cortex and amygdala, respectively. Scale bar represents 2 mm. ***b***, PCR detection of vector genome (IVa2), transgene (TK) or replication-competent genome (E1B), in brain sections of rats that were treated with Rad128 and Rad127 and survived for 90 days. A PCR product corresponding to the Ad 5 IVa2 primary transcript was amplified from brains injected with RAd127 and RAd128 3 months earlier (lanes 5 and 6), or from brains injected 3 d earlier with a different vector preparation contaminated with a replication-competent adenovirus (lane 4). A PCR product corresponding to the Ad 5 E1B primary transcript was amplified from brains injected with the viral preparation contaminated with replication competent virus (lane 4), and from genomic DNA from 293 cells (lane 2). A PCR product, TK, which can be amplified from both genomic sequences encoding either HSV-1-TK or HSV-1-ΔTK, was amplified from brains injected with RAd127 and RAd128 3 months earlier (lanes 5 and 6). Controls, Sterile water (lane 1) and a brain section from a rat not injected with any viral vector (lane 3). Right margin, molecular sizes. ***c***, Regions amplified by PCR. Top, The left 6,000 base pairs of the Ad 5 genome, and the transcription units for E1A, E1B and IVa2. Middle, Ad 5 sequence in 293 cells. Bottom, Ad 5 sequence in RAd127 and RAd128, and site at which the transcription unit is inserted. Short arrows, sites of amplification for primer pairs a/b, c/d and e/f.

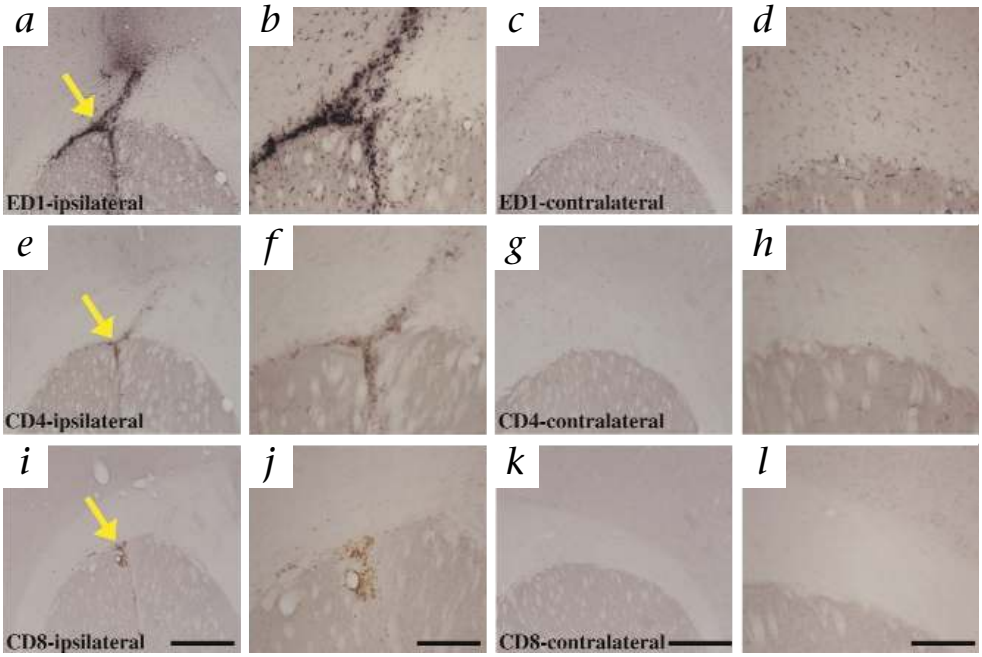

Fig. 6 Immune-mediated elimination of CNS-1 cells does not lead to chronic persistent infiltration of $CD4^+$ or $CD8^+$ T cells. Peripheral priming with mitomycin C treated CNS-1 cells prevents intracranial tumor growth and does not induce a chronic inflammatory response in the rat brain after the intrastriatal injection of control CNS-1 cells into the ipsilateral striatum. Vibratome sections were stained and photographed at low magnification (*a*, *e*, *I*, *c*, *g* and *k*), and at higher magnification (*b*, *f*, *j*, *d*, *h* and *l*). Tumor growth is not evident in the ipsilateral hemisphere of the brains injected with CNS-1 cells 30 days after a peripheral priming with mitomycin C-treated CNS-1 cells (*a*, *b*, *e*, *f*, *I* and *j*). ***a*–*d***, ED1-stained brains show microglial/macrophage activation (yellow arrow, *a*), limited to the white matter and the striatum. ED1-positive cells are present at a reduced level in the white matter of the contralateral hemisphere (*c* and *d*). ***e*–*h***, CD4-stained sections do not show specific staining for CD4-positive T lymphocytes (*e* and *f*), although CD4-labeled microglial cells can be detected. ***i*–*l***, CD8-stained sections do not show specific staining for CD8-positive T lymphocytes throughout the area of tumor injection, although occasional lymphocytes normally present within the meninges are stained. The remains of oxidized red blood cells can be seen at the site of tumor implantation (yellow arrow, *i*). Scale bars represent 1 mm (for *a*,*e*,*I*,*c*,*g*,*k*; shown in *I* and *k*) and 0.5 mm (for *b*,*f*,*j*,*d*,*h*,*l*; shown in *j* and *l*).

RAd128 and ganciclovir cause persistent lymphocyte infiltration

To determine whether the chronic lymphocyte infiltration and inflammation was caused by the elimination of CNS-1 cells, the administration of viral vectors expressing HSV-1-TK or the subsequent administration of ganciclovir, we tested these variables independently. Peripheral priming of Lewis rats with 2.5×10^4 mitomycin-C treated CNS-1 cells protected rats from a lethal intracerebral challenge with 5×10^3 CNS-1 cells. We perfusion-fixed surviving rats 90 days after the intracerebral challenge. No tumor, $CD8^+$ or $CD4^+$ cells could be detected (Fig. 6). We only detected a small increase in $ED1^+$ macrophages/microglial cells, compared with that after the inhibition of tumor growth by gene therapy (Figs. 2*g* and *h* and 6*a* and *b*). Thus, immune-mediated elimination of CNS-1 cells does not lead to a prolonged infiltration of lymphocytes into the brain. Intracerebral injection of 8 x 10^7 IU of RAd-128 in the absence of CNS-1 cells, followed by administration of ganciclovir or saline for 7 days, and perfusion-fixation 1 or 3 months later, led to a chronic brain inflammatory infiltration, with higher numbers of $CD8^+$ lymphocytes in rats treated with ganciclovir (Fig. 7).

Discussion

We made three main findings during our conditional cytotoxic gene therapy studies in a syngeneic rat glioblastoma model: Complete tumor growth inhibition in most rats; a chronic, ongoing, inflammatory process, characterized by T-cell and macrophage/microglial infiltration and activation, and loss of myelinated fibers and axons in long-term survivors; and continued expression of transgenic HSV-1-TK at very high levels in neurons throughout the brains of survivors 90 days after vector administration. We have reported chronic active inflammation in response to a single, successful, brain glioma gene therapy regime, and the long-term presence of the therapeutic enzyme HSV-1-TK. Furthermore, we have demonstrated that the chronic inflammatory process does not impair long-term transgene expression in the brain. As the presence of HSV-1-TK throughout the contralateral cortex and striatum did not result in overt local inflammatory responses, additional mechanisms will have to be invoked to explain the usual short-lived transgene expression after adenovirus vector-mediated gene transfer to the brain[18–21,23,24].

Most experimental models of glioblastoma gene therapy have used C6, 9L or F98 glioma cells[8–17], and have failed to report any chronic inflammatory responses. After a single administration of adenovirus encoding the marker gene β-galactosidase or HSV-1-TK to either rats, mice, nonhuman primates or human glioma, mainly acute, short-lived and dose-dependent inflammatory responses have been described so far[18–21,23,24,28–30]. The ongoing nature of the inflammatory process detected in our model is supported by our finding of perivascular cuffs, composed of both T cells and activated microglia/macrophages. The injection volumes, viral and ganciclovir doses, and our experimental paradigm are within the ranges described in the literature[8–17]. However, we have reported here a syngeneic glioma gene therapy model in Lewis rats, which are highly susceptible to experimental allergic encephalomyelitis[31].

So far, localized demyelination has been described only after the peripheral readministration of adenovirus vectors[19]. Moreover, in our experiments, the chronic inflammatory response was also limited to the hemisphere originally injected with tumor cells and viruses. We detected no inflammatory responses at any distant sites expressing high levels of immunoreactive HSV-1-TK. Further, our data demonstrated a loss of myelinated fibers, edema, and indices of ongoing axonal degeneration, whereas oligodendrocytes were preserved and primary demyelinated axons were absent. This demonstrates that the loss of myelinated fibers, is not primary, or immune-mediated, but secondary to tissue injury and axonal loss.

Adenovirus injection into brain parenchyma stimulates the secretion of interleukin (IL)-1 and IL-6, whereas injection into the lat-

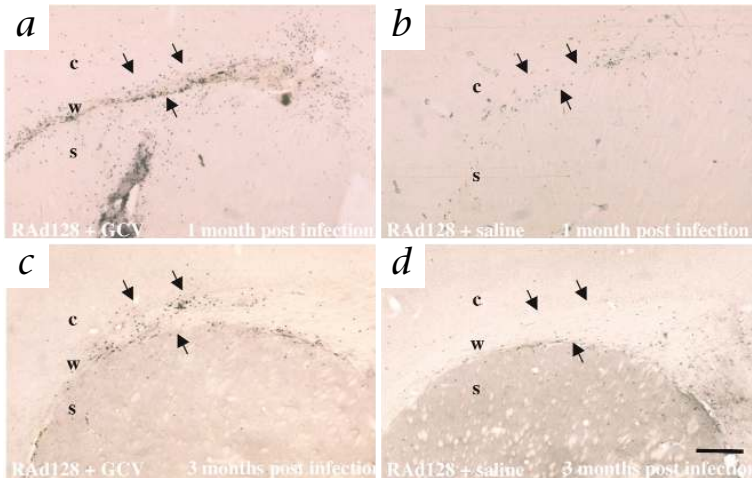

Fig. 7 Injection of RAd-128 followed by ganciclovir leads to chronic sustained infiltration of CD8⁺ T cells. Injection of the same dose of RAd-128 that was used to inhibit tumor growth leads to a stronger infiltration of CD8⁺ lymphocytes at 1 and 3 months after injection, if rats were treated with ganciclovir, but not saline, twice daily for 7 days. Arrows, boundaries of the white matter showing T-cell infiltration. c, cortex; w, white matter; s, striatum. Scale bar represents 450 μm.

eral ventricle induces secretion of IL-1, IL-6 and tumor necrosis factor-α (ref. 20). Thus, the immune-suppressive microenvironment of the brain and gliomas (which express transforming growth factor-β (ref. 32) and Fas ligand[33]) could be modified by viral-mediated gene therapy, through the secretion of pro-inflammatory cytokines, coupled with inflammation elicited through HSV-1-TK and ganciclovir-mediated cell killing. This could enhance tumor immunogenicity and improve gene therapy's anti-tumor activity.

The persistent inflammation is not exclusively due to the elimination of CNS-1 cells, as the subcutaneous priming with growth-arrested CNS-1 cells completely protected rats from an intracerebral challenge, without leading to a chronic inflammatory response. Thus, immune system-mediated elimination of glioma cells (as opposed to adenovirus-mediated gene therapy) does not lead to chronic inflammation and lymphocyte infiltration. However, injection of RAd-128 followed by ganciclovir administration did cause a substantial influx of CD8⁺ cells, which was much reduced in the absence of ganciclovir treatment. Thus, the persistent inflammation is a result of the combined effect of HSV-1-TK and ganciclovir, but is not a direct result of the elimination of the tumor cells itself. Whether this effect will be shown to be specific to adenovirally encoded HSV-1-TK, or whether it will be seen when HSV-1-TK is expressed by other viral vectors remains to be determined.

Another important finding was the widespread presence of immunoreactive HSV-1-TK within ipsilateral and contralateral neocortex and striatum, as well as within ipsilateral glia and inflammatory cells 3 months after vector injection and ganciclovir administration. So, HSV-1-TK immunoreactive cells either became infected after the administration of ganciclovir or are resistant to HSV-1-TK plus ganciclovir-dependent cytotoxicity. HSV-1-immunoreactive neurons had normal morphologies, indicating that the long-term presence of HSV-1-TK and ganciclovir administration did not compromise neuronal survival. This contrasts with sympathetic neurons in culture, in which infection with adenovirus vectors leads to neuronal death in a few days[34]. Our findings also contrast with published experiments describing much more anatomically restricted adenoviral encoded neuronal protein expression[18,19,21–24].

The presence of HSV-1-TK throughout the ipsilateral and contralateral neocortex was restricted to pyramidal neurons, mainly located in layers II–II and V, which contain callosally and cortico–cortically projecting pyramidal cells. Such neurons may have taken up vectors through axonal varicosities present on axons coursing throughout the subcortical white matter overlying the injected striatum[35]. Alternatively, HSV-1-TK protein could have been released by dying cells (if spared from intracellular degradation) and taken up by axonal terminals to be transported retrogradely to parent neuronal cell bodies. This is unlikely, however, given the widespread distribution of HSV-1-TK protein and viral vector genomes in distant cells, including neurons, throughout the brain. The presence of vector genomes but the absence of replication-competent virus from brains of long-term survivors indicates the apparent stability of and long-term expression from adenoviral vectors injected into the rodent brain.

Despite of aggressive surgery, chemotherapy and radiotherapy, median survival of glioblastoma patients is less than 12–15 months, and has not improved during the last 30 years. This calls for new treatments, such as gene therapy. All current treatments have considerable side effects. Surgery can damage vital brain areas, chemotherapy has very high toxicity, and widespread demyelination is a long-term consequence of radiotherapy.

Several clinical trials of glioblastoma suicide gene therapy using retroviruses and adenoviruses encoding HSV-1-TK, in combination with ganciclovir, are now ongoing[1–4]. Our work has implications for clinical trials of glioblastoma gene therapy using adenoviruses expressing HSV-1-TK: effective gene transfer may occur to as-yet unexpectedly widespread areas of the human brain; the development of a chronic inflammatory response in humans could lead to a loss of myelinated fibers; and long-term persistence of HSV-1-TK could lead to improvements in the clinical trial's schedule of ganciclovir administration. Extending the administration of ganciclovir could improve the anti-tumor effect by allowing killing of transduced glioma cells that have not yet entered the cell cycle during short periods of post-surgical ganciclovir administration now in use. The severity of gene therapy's untoward effects will have to be balanced with its increased anti-glioblastoma efficiency, in relation to the limitations of therapies now in use.

Methods

Cell culture. The rat glioma cell line CNS-1 was provided by W. Hickey (Dartmouth Medical Center, Department of Pathology, Lebanon, New Hampshire)[25]. The kidney embryonic cell line 293 was obtained from Microbix Biosystems (Toronto, Canada). The maintenance of the cell lines has been described[36,37].

Adenovirus vectors expressing HSV-1-TK, HSV-1-ΔTK, or β-galactosidase. RAd vectors encoding HSV-1-TK (RAd-128) and HSV-1-ΔTK (RAd-127) under control of the short immediate–early human cytomegalovirus (sMIEhCMV) promoter[36,37] were generated and characterized as described (ref. 27 and R.A.D. *et al.*, manuscript submitted). Viruses were purified using double-cesium chloride gradients, and titers of 1×10^{10}–1×10^{11} infectious units (IU)/ml, and particle/plaque-forming unit ratios of 30 were obtained as described[17,20,27,36,37]. An adenovirus purified by double-cesium chloride gradient, RAd-35, expressing the *Escherichia coli* β-galactosidase gene driven by the sMIEHCMV promoter, was used as a control virus[37]. *In vitro*, CNS-1 cells do express the transgene HSV-1-TK after infection with adenoviral vectors, and are sensitive to apoptosis induced after the addition of ganciclovir to infected cultures[27].

Lipopolysaccharide endotoxin (LPS) assay and replication-competent adenovirus assays. LPS contamination in each RAd stock was assessed by using the amebocyte horseshoe crab lysate method (E-Toxate assay; Sigma)[38]. RAd-127 and RAd-128 had levels of LPS less than 5 milli-endotoxin units (mEU)/μl; thus, in the 4 μl injected, total LPS was less than 20 mEU. β-galactosidase-expressing RAd-35 had levels of LPS ≤ 2 mEU/μl; thus, in the 4 μl injected, total LPS was ≤ 8 mEU. The amount of LPS needed to produce inflammatory responses in the brain is several-fold more than the upper limit of bioactive LPS activity value obtained in our bio-assays[39]. Our viral volumes injected were essentially LPS-free. The presence of replication-competent adenovirus was tested by the supernatant rescue assay[40]. No replication-competent adenovirus was detected in 2.6×10^8 IU of either of the RAd-127 and RAd-128 vector stocks used in our experiments, showing the absence of replication-competent adenovirus in an amount of vector three times higher than the total amount of infectious units that were injected *in vivo*.

***In vivo* treatment of gliomas**. Male Lewis rats (250–300 g in body weight) were anesthetized with halothane (Zeneca, Macclesfield, UK) and placed in a stereotaxic frame. A burr hole in the skull was made with a drill 3 mm to the right of and 1 mm anterior to the bregma. A 5-μl syringe fitted with a 26-gauge needle was connected to the manipulating arm of a stereotaxic frame, and 5×10^3 or 10×10^3 CNS-1 cells (in 3 μl phosphate-buffered saline; PBS) were injected over a 3-minute period into the striatum at the following location: bregma +1 mm; lateral +3 mm; ventral –4 mm. The needle was left in place for another 5 min before being removed.

Viruses were injected into the tumor site 3 d after tumor implantation. Using the same anterior and lateral coordinates, 1 μl PBS or 1 μl (2×10^7 IU/μl) RAd-127, RAd-128 or RAd-35 were injected at each of the following ventral coordinates: –5mm; –4.5mm; –4mm; –3.5mm. Starting 12 h after the injection of the viral vector, 25 mg/kg ganciclovir (Cymevene; Roche Products, Welwyn Garden City, UK) was injected intra-peritoneally twice daily for 7 d. Rats injected with RAd-127, RAd-128, RAd-35 or PBS (n = 5 per group) were monitored daily. Any rat showing any sign of morbidity was perfusion-fixed, and brains were removed for histological analysis.

In other groups of rats not implanted with CNS-1 tumors, the same amount of RAd-128 was injected into the brain, and was followed by administration of ganciclovir or saline for 7 d (n = 3 per group). Rats were perfused either at 1 or 3 months after adenoviral vector injection.

Histological analysis, fixation, paraffin and plastic sections. Rats were anesthetized, and fixed by cardiac perfusion. First, rats were perfused with approximately 200 ml Tyrode solution (0.14 M NaCl, 2.7 mM KCl, 1.8 mM $CaCl_2$, 0.32 mM NaH_2PO_4, 5.6 mM glucose and 11.6 mM $NaHCO_3$), containing 10 units/ml heparin (CP Pharmaceuticals, Wrexham, UK). This was followed by 250 ml of 4% paraformaldehyde in PBS, pH 7.4. Brains were removed and placed in 4% paraformaldehyde for 24 h. Serial Vibratome sections (70 μm in thickness) were maintained at 4 °C in PBS. Sections were stained with hematoxylin and eosin or by Luxol fast blue, or were processed for immunohistochemistry. Alternatively, some rats were perfused with 1% glutaraldehyde and 2% paraformaldehyde in 0.1 M phosphate buffer, pH 7.4, and post-fixed for 2–3 d. Some of the paraformaldehyde-fixed brains were dissected, and tissue blocks containing the needle track were embedded on paraffin. Serial sections were made from each block to define precisely the location of the injection area. Paraffin sections 5 μm in thickness were stained with hematoxylin and eosin, with Luxol fast blue myelin stain and with Bielschowski silver impregnation for axons. Immunocytochemistry used the avidin–biotin technique, with the following primary antibodies: W3/13 (leucosyalin, mouse monoclonal staining of rat T cells) and OX8 (mouse monoclonal antibodies recognizing $CD8^+$ T lymphocytes)(both from Serotec, Raleigh, North Carolina); and cyclic nucleotide phosphodiesterase (CNPase; mouse monoclonal SMI 91). Glutaraldehyde-fixed tissue was dissected into small tissue blocks containing the injection site. Material was then further fixed and stained in 1% osmic acid in PBS, and embedded into Epon; 0.5-μm thick plastic sections were stained with toluidine blue.

Immunohistochemistry on vibratome sections. Immunohistochemistry was done on free-floating sections, as described[35,41]. Antibodies against GFAP (Boehringer) and vimentin (Sigma), specific for astrocyte-specific intermediate filaments, were used to identify astrocytes; and β-tubulin III (Sigma, Poole, Dorset, UK), to detect neurons and their axons. Antibodies against ED1, to identify monocytes/macrophages/microglial cells, antibodies against CD3 to detect total lymphocytes, and antibodies against CD8, which detect CD8 positive lymphocytes and natural killer cells, and antibodies against CD4, were from Serotec (Raleigh, North Carolina). HSV-1-TK proteins were detected using a polyclonal antibody against HSV-1-TK (provided by M. Janicot, Rhone Poulenc Rorer, Paris, France). Sections were washed twice with Tris-buffered saline (TBS: 50 mM Tris, 0.9% NaCl and 0.5% Triton, pH 7.4), incubated for 15 min with 0.3% H_2O_2, washed three times with 2 ml of TBS, incubated for 45 min with 10% normal horse serum (NHS; Life Technologies) in TBS, and washed briefly for 10 min with 1% NHS in TBS. Sections were then incubated overnight at room temperature with primary antibodies at the following dilutions in 1% NHS in TBS: antibody against GFAP (1:200), monoclonal antibody against vimentin clone V9 (1:1,000), antibody against ED-1 (1:1,000), antibody against CD3 (1:500), antibody against CD4 (1:200), antibody against CD8 (1:500), antibody against β-tubulin III (1:2,000), and polyclonal antibody against HSV-1-TK (1:1,000). The next day, sections were washed three times with TBS before being incubated for 4 h at room temperature with a 1:200 dilution of the secondary antibody (rabbit antibody against mouse immunoglobulins or swine antibody against rabbit immunoglobulins, biotinylated; Dako, Carpinteria, California). Sections were then washed three times with TBS before being incubated for 3 h at room temperature with avidin–biotin complex (Vectastain ABC Kit; Vector Laboratories, Bretton, Peterborough, UK). Subsequently, sections were washed three times with PBS and two additional times with 0.1 M acetate buffer, pH 6. Staining was developed by incubating the sections for 5 min at room temperature with a solution containing equal volumes of 0.2 M acetate buffer pH 6 containing 48 g/l ammonium nickel sulphate, 4 g/l glucose, 0.8 g/l ammonium chloride, and 1 g/l 3,3′-diaminobenzidine and 50 mg/l glucose oxidase in distilled water. The staining reaction was stopped by washing the sections two times in 0.1 M acetate buffer, pH 6, and two additional times in PBS. Sections were placed on gelatin-coated slides, dehydrated, coverslipped and mounted.

Statistical analysis. Survival data were analyzed by Kaplan-Meier estimator analysis, and compared using the generalized Wilcoxon test with the Prentice-Peto algorithm.

Magnetic resonance imaging. Proton magnetic resonance imaging of the rat brain used a 4.7-T, 15-cm horizontal bore Biospec (Bruker Spectrospin, Conventry, UK) system, using a 2.5-cm surface coil. During imaging, rats were kept anesthetized with general anesthesia by means of a gas mixture of halothane (Zeneca, Macclesfield, UK) and oxygen. To detect tumors in the brain, axial images, slices 2 mm in thickness, were acquired at approximately 2-mm intervals. The position of the slice of interest, relative to the plane of coil, was selected by applying a 90° 'hard' pulse between 35 and 90 μs in duration. In preliminary studies, T_1, T_2, magnetization transfer contrast and diffusion-weighted pulse sequences were compared to determine the conditions required to give optimum contrast between tumor and normal brain tissue. Although the tumors were detectable in T_2-weighted images, magnetization transfer contrast[42,43] provided greater contrast and was used in all subsequent experiments. The magnetization transfer contrast sequence involved the application of a pulse of radiation of 1-s duration, with an offset of 5 kHz and an amplitude of 15 μT. In-plane resolution was 240- × 480-μm for a field of view of 6.2 cm. The superiority of this imaging technique in the detection of gliomas has been demonstrated[44].

Detection of adenoviral genome in brain sections using PCR. Adenoviral sequences were detected in free-floating vibratome-cut brain sections using polymerase chain reaction (PCR). Sections were digested for 24 h at 37 °C in 10 mM Tris-HCl, pH 8, 10 mM NaCl, 25 mM EDTA, 1% SDS and 4 mg/ml proteinase K. The proteinase K was heat-inactivated at 95 °C for 10 min, after which two rounds of phenol:chloroform:isoamyl alcohol (25:24:1) extraction were done. The genomic DNA was then ethanol-precipitated with 3 M sodium acetate, pH 5.2, washed with 70% ethanol and then re-suspended in sterile water contaning 20 μg/ml DNase-free RNase.

Sequences of Ad 5 transcription unit IVa2, Ad 5 E1B, HSV—1 TK and β-actin were detected using four different primer sets. Primers a and b (Fig. 5*c*) are specific to the IVa2 transcription unit of the Ad 5 genome and produce a PCR product of 687 bp. Primers c and d (Fig. 5*c*) are specific to the E1B transcription unit of the Ad 5 genome and produce a PCR product of 561 bp (ref. 34). Primers e and f (Fig. 5 c) are specific to HSV-1 TK and produce a PCR product of

365 bp from TK and ΔTK. Primers g and h have been modified from a method for detecting chicken β-actin[45] and produce a PCR product of 340 bp from exon 4 of rat cytoplasmic β-actin. In a 50-μl PCR reaction, 5–10 μl genomic DNA was used in a solution containing 1X PCR buffer (Promega), 200μM dATP, 200 μM dTTP, 200 μM dCTP, 200 μM dGTP, 2 mM $MgCl_2$, 2 ng/μl each primer and 1U *Taq* polymerase (Promega). PCR conditions comprised 35 cycles of 30 s of denaturation, 30 s of annealing, and a 1-minute extension followed by another 10 min of extension. The annealing temperatures for primer pairs a/b, c/d, e/f and g/h were 56 °C, 57 °C, 63 °C and 63 °C, respectively. The PCR products were separated by 2% agarose gel electrophoresis and were visualized on a UV transilluminator after being stained with ethidium bromide. Primer sequences were a, 5′–AAGCAAGTGTCTTGCTGTCT–3′; b, 5′–GGATGGAACCATTATACCGC–3′; c, 5′–CAAGAATCGCCTGCTACTGTTGTC–3′; d, 5′–CCTATCCTCCGTATCTATCTCCACC–3′; e, 5′–AAAACCACCACCACGCAACT–3′; f, 5′–GTCATGCTGCCCATAAGGTA–3′; g, 5′–CCAGCCATGTACGTAGCCATCC–3′; h, 5′–GCAGCTCATAGCTCTTCTCCAGG–3′.

Peripheral priming with CNS-1 cells. CNS-1 cells were treated with 2 μg/ml mitomycin C overnight to arrest cell division. Either 2.5×10^4 mitomycin C-treated CNS-1 cells (for primed rats) or PBS (for control rats) were injected subcutaneously into the flanks of Lewis rats ($n = 4$ per group). Then, 30 d later, all rats were re-challenged by implantation of 5×10^3 CNS-1 cells into the striatum, unilaterally. All rats primed peripherally with mitomycin C-treated CNS-1 cells survived, whereas those primed with PBS died by day 30 after tumor implantation. Surviving rats were perfused 90 d after intracerebral challenge.

Acknowledgments

The technical assistance of T. Maleniak and the secretarial help of Ros Poulton, are acknowledged. We also thank I. Miller and T. Bentley from the Electron Microscopy, Photography and Graphics Unit (School of Biological Sciences, University of Manchester) for their help and advice with the final production of the figures. Comments on the work and manuscript by D. Mann, and P. Kingston are acknowledged. This work was supported by Cancer Research Campaign, UK (project grant number SP2332/0101 to P.R.L. and M.G.C.), and European Community Biomed II grant to P.R.L., M.G.C. and D.K. (Contract number BMH4-CT96-1436). T.D.S. is an Action Research Training Fellow, and P.R.L. is a Research Fellow of The Lister Institute of Preventive Medicine.

RECEIVED 16 AUGUST; ACCEPTED 15 SEPTEMBER 1999

1. Izquierdo, M. *et al.* Human malignant brain tumour response to herpes simplex tymidine kinase *(HSVtk)*/ganciclovir gene therapy. *Gene Therapy* **3**, 491–495 (1996).
2. Ram, Z. *et al.* Therapy of malignant brain tumors by intratumoral implantation of retroviral vector-producing cells. *Nature Medicine* **3**, 1354–1361 (1997).
3. Klatzmann, D. *et al.* A phase I/II study of herpes simplex virus type 1 thymidine kinase "suicide" gene therapy for recurrent glioblastoma. *Hum. Gene Ther.* **9**, 2595–2604 (1998).
4. Eck, S.L. *et al.* Treatment of advanced CNS malignancies with the recombinant adenovirus H5.010RSVTK: a phase I trial. *Hum. Gene Ther.* **7**, 1465–1482 (1996).
5. Freeman, S. *et al.* The "bystander effect": tumour regression when a fraction of the tumour mass is genetically modified. *Cancer Res.* **53**, 5274–5283 (1993).
6. Freeman, S.M., Ramesh, R. & Marrogi, A.J. Immune system in suicide gene therapy. *Lancet* **349**, 2–3 (1997)
7. Gagandeep, S. *et al.* Prodrug-activated gene therapy: involvement of an immunological component in the "bystander effect". *Cancer Gene Ther.* **3**, 83–88 (1996).
8. Barba, D., Hardin, J., Sadelain, M. & Gage, F. Development of anti-tumor immunity following thymidine kinase-mediated killing of experimental brain tumors. *Proc. Natl. Acad. Sci. USA* **91**, 4348–4352 (1994).
9. Beck, C., Cayeux, S., Lupton, S., Dorken, B. & Blankenstein, T. The thymidine kinase/ganciclovir-mediated "suicide" effect is variable in different tumour cells. *Hum. Gene Ther.* **6**, 1525–1530 (1995).
10. Chen, S.-H., Shine, H.D., Goodman, J., Grossman, R. & Woo, S.L.C. Gene therapy for brain tumors: regression of experimental gliomas by adenovirus-mediated gene transfer *in vivo. Proc. Natl. Acad. Sci. USA* **91**, 3054–3057 (1994).
11. Culver, K. *et al. In vivo* gene transfer with retroviral vector-producer cells for treatment of experimental brain tumors. *Science* **256**, 1550–1552 (1992).
12. Ezzeddine, Z. *et al.* Selective killing of glioma cells in culture and in vivo by retrovirus transfer of the herpes simplex virus thymidine kinase gene. *New Biologist* **3**, 608–614 (1991).
13. Izquierdo, M. *et al.* Long-term rat survival after malignant brain tumor regression by retroviral gene therapy. *Gene Ther.* **2**, 66–69 (1995).
14. Maron, A. *et al.* Gene therapy of rat C6 glioma using adenovirus-mediated transfer of the herpes simplex virus thymidine kinase gene: long-term follow-up by magnetic resonance imaging. *Gene Therapy* **3**, 315–322 (1996).
15. Perez-Cruet, M. *et al.* Adenovirus-mediated gene therapy of experimental gliomas. *J. Neurosci. Res.* **39**, 506–511 (1994).
16. Ram, Z. *et al.* The effect of thymidine kinase transduction and ganciclovir therapy on tumor vasculature and growth of 9L giomas in rats. *J. Neurosurg.* **81**, 256–260 (1994).
17. Ambar, B.B. *et al.* Treatment of experimental glioma by administration of adenoviral vectors expressing Fas ligand. *Hum. Gene Ther.* **10**, 1641–1648 (1999).
18. Byrnes, A.P., Rusby, J.E., Wood, M.J.A. & Charlton, H.M. Adenovirus gene transfer causes inflammation in the brain. *Neuroscience* **66**, 1015–1024 (1995).
19. Byrnes, A.P., MacLaren, R.E. & Charlton, H.M. Immunological instability of persistent adenovirus vectors in the brain: peripheral exposure to vector leads to renewed inflammation, reduced gene expression, and demyelination. *J. Neurosci.* **16**, 3045–3055 (1996).
20. Cartmell, T. *et al.* IL-1 mediates a rapid inflammatory response following adenoviral vector delivery into the brain. *J. Neurosci.* **19**, 1517–1523 (1999).
21. Geddes, B.J., Harding, T.C., Lightman, S.L.& Uney, J.B. Long-term gene therapy in the CNS: reversal of hypothalamic diabetes insipidus in the Brattleboro rat by using an adenovirus expressing arginine vasopressin. *Nature Med.* **3**, 1402–1404 (1997).
22. Ghodsi, A. *et al.* Extensive β-glucuronidase activity in murine central nervous system after adenovirus-mediated gene transfer to brain. *Hum. Gene Ther.* **9**, 2331–2340 (1998).
23. Blomer, U., Naldini, L., Kafri, T., Trono, D., Verma, I.M. & Gage, F.H. Highly efficient and sustained gene transfer in adult neurons with a lentivirus vector. *J. Virol* **71**, 6641–6649 (1997).
24. Hermens, W.T. & Verhaagen, J. Suppression of inflammation by dexamethasone prolongs adenoviral vector-mediated transgene expression in the facial nucleus of the rat. *Brain Res. Bull.* **47**,133–40 (1998).
25. Kruse, C.A. *et al.* A rat glioma model, CNS-1, with invasive characteristics similar to those of human gliomas: a comparison to 9L gliosarcoma. *J. Neurooncol.* **22**, 191–200 (1994).
26. Salomon, B *et al.* A truncated herpes simplex virus thymidine kinase phosphorylates thymidine and nucleoside analogs and does not cause sterility in transgenic mice. *Mol. Cell. Biol.* **15**, 5322–5328 (1995).
27. Dewey, R.A. *et al.* Adenoviral-mediated suicide gene therapy using the CNS-1 rat glioma model. *Abstr. Soc. Neurosci.* Part 2 **2165**, number 859.9 (1998).
28. Goodman, J. *et al.* Adenoviral-mediated thymidine kinase gene transfer into the primate brain followed by systemic ganciclovir: pathologic, radiologic, and molecular studies. *Hum. Gene Ther.* **7**, 1241–1250 (1996).
29. Smith, J. *et al.* Intracranial administration of adenovirus expressing HSV-TK in combination with ganciclovir produces a dose-dependent, self-limiting inflammatory response. *Hum. Gene Ther.* **8**, 943–954 (1997).
30. Puumalainen, A. *et al.* Beta-galactosidase gene transfer to human malignant glioma in vivo using replication-deficient retroviruses and adenoviruses. *Hum. Gene Ther.* **9**, 1769–1774 (1998).
31. Klinkert, W.E. *et al.* TNF-alpha receptor fusion protein prevents experimental auto-immune encephalomyelitis and demyelination in Lewis rats: an overview. *J. Neuroimmunol.* **72**, 163–168 (1997).
32. Weller, M. & Fontana, A. The failure of current immunotherapy for malignant glioma. Tumor-derived TGF-beta, T-cell apoptosis, and the immune privilege of the brain. *Brain Res. Brain Res. Rev.* **21**, 128–151 (1995).
33. Gratas *et al.* Fas ligand expression in glioblastoma cell lines and primary astrocytic brain tumours. *Brain Pathol.* **7**, 863–869 (1997).
34. Easton, R.M., Johnson, E.M. & Creedon, D.J. Analysis of events leading to neuronal death after infection with E1-deficient adenoviral vectors. *Mol. Cell. Neurosci.* **11**, 334–347 (1998).
35. Shering, A.F. & Lowenstein, P.R. Neocortex provides direct synaptic input to interstitial neurons of the intermediate zone of kittens and white matter of cats: a light and electron microscopic study. *J. Comp. Neurol.* **347**, 433–443 (1994).
36. Morelli, A. *et al.* Reduced systemic toxicity of recombinant adenovirus vectors expressing the apoptotic molecule Fas-L driven by cell-type specific promoters. *J. Gen. Virol.* **80**, 571–583 (1999).
37. Shering, A.F. *et al.* Cell-type specific expression in brain cell cultures from a short human cytomegalovirus major immediate early promoter depends on whether it is inserted into herpesvirus or adenovirus vectors. *J. Gen. Virol.* **78**, 445–459 (1997).
38. Cotten, M., Baker, A., Saltik, M., Wagner, E. & Buschle, M. Lipopopysaccharide is a frequent contamination of plasmid DNA preparations and can be toxic to primary human cells in the presence of adenovirus. *Gene Ther.* **1**, 239–246 (1994).
39. Hauss-Wgrzyniak, B., Lukovic, L., Bigaud, M. & Stoeckel, M.E. Brain inflammatory response induced by intracerebroventricular infusion of lipopolysaccharide: an immunohistochemical study. *Brain Res.* **794**, 211–224 (1998).
40. Dion, D. L., Fang, J. & Garver Jr., R. I. Supernatant rescue assay vs. polymerase chain reaction for detection of wild type adenovirus-contaminating recombinant adenovirus stocks. *J. Virol. Meth.* **56**:99–107 (1996).
41. Lowenstein, P.R., Shering, A.F., James, J.L., Cohen, P. & McDougall, L. The distribution of protein phosphatase inhibitor, Inhibitor 1, in the neocortex of the cat, ferret, and rat: a light and electron microscopical study. *Brain Res.* **676**, 80–92 (1995).
42. Wolff, SD & Balaban, RS. Magnetization transfer contrast (MTC) and tissue water proton relaxation *in vivo. Magn. Reson. Med.* **10**, 135–144, 1989
43. Wolff, S.D. & Balaban, R.S. Magnetization transfer imaging: practical aspects and clinical applications. *Radiology* **192**, 593–599, 1994.
44. Kurki, T., Lundbom, N., Kalimo, H. & Valtonen, S. MR classification of brain gliomas: value of magnetization transfer and conventional imaging. *Magn. Reson. Imaging* **13**, 501–511 (1995).
45. Lee, K.H. & Contache, D.A. Detection of β-actin mRNA by RT-PCR in normal and regenerating chicken cochleae. *Hearing Res.* 87, 9–15 (1995).